Biointerface Research in Applied Chemistry
Platinum Open Access Journal (ISSN: 2069-5837)

Article
Volume 10, Issue 5, 2020, 6427 - 6435
https://doi.org/10.33263/BRIAC105.64276435

Electronic Properties of Polyvinyl Alcohol/ TiO_2/SiO_2 Nanocomposites

Rania Badry [1], Asmaa Ibrahim [1], Fatma Gamal [1], Dina Shehata [1], Hend Ezzat[2], Hanan Elhaes[1], Medhat Ibrahim [3,*]

[1] Physics Department, Faculty of Women for Arts, Science and Education, Ain Shams University, 11757 Cairo, Egypt
[2] Nano Technology Unit, , Solar and Space Research Department, National Research Institute of Astronomy and Geophysics (Nano NRIAG), 11731 Helwan, Cairo, Egypt
[3] Molecular Spectroscopy and Modeling Unit, Spectroscopy Department, National Research Centre, 33 El-Bohouth St., 12622 Dokki, Giza, Egypt
* Correspondence: medahmed6@yahoo.com;

Scopus Author ID 8641587100
Received: 5.04.2020; Revised: 6.05.2020; Accepted: 10.05.2020; Published: 13.05.2020

Abstract: Molecular modeling shows potential applications for calculating physical as well as chemical parameters of many molecular systems. Physical parameters such as HOMO-LUMO band gap energy (ΔE), total dipole moment (TDM) and the molecular electrostatic potential (MESP) are reflecting the reactivity of the given chemical structure. So, the effect of titanium dioxide (TiO_2) and silicon dioxide (SiO_2) upon Polyvinyl chloride PVC is studied in terms of physical properties. Such parameters were calculated with density functional theory: B3LYP using LANL2DZ basis set. Model molecules for PVA, TiO_2, SiO_2, PVA/TiO_2, PVA/SiO_2 and PVA/TiO_2/SiO_2 were optimized then ΔE, TDM and MESP were calculated at B3LYP/LANL2DZ. The results indicated that the reactivity of PVA is improved as a result of interaction with TiO_2 and SiO_2.

Keywords: TiO_2; SiO_2; PVA; HOMO/LUMO energy; TDM; MESP.

1. Introduction

Material science is classified as an interdisciplinary field having common interest to wide range of researchers not limited to physicists, chemists, and engineers. Studying basic principles of materials has been one of the most challenging attempts of science and technology. Electronic properties of materials are now playing a crucial role in clarifying the functionality of materials. These properties are ranging from microscopic such as band structure to macroscopic resistivity, conductivity, mass effectivity, permittivity. According to physical as well as chemical properties importance, as it became necessary for characterization and classification of materials [1-5].

Investigating the electronic properties could be achieved with many routes including both experimental and theoretical. Accordingly, molecular modeling at different levels shows potential applications for investigating electronic properties for wide range of materials and in different fields of applications [6-12]. Modeling could provide important data for many systems whereas the experimental setup is limited and/or unavailable. Polyvinyl chloride PVC is one of the cheapest and easiest handled synthetic polymers [13-15]. It is widely applied in many applications despite its amorphous nature [16]. It could be reshaped, blended with other metal oxides in order to enrich their properties and increase its functionality for many applications

[17-20]. This leads to the fact that PVC as well as its derivatives are among the most common polymers worldwide [21]. Meanwhile, it could be recycled and reprocessed which gives it commercial values [22]. Nowadays, it is common to apply PVC derivatives as nanocomposite for modern applications including gas sensors [23-24]. The effect of metal oxides on the PVC nanocomposite was followed up with molecular modeling to study geometrical as well as different physical properties [25]. As the topic still of concern this work is conducted. DFT at B3LYP/ LANL2DZ level was used to evaluate the electronic properties of PVA, PVA/TiO_2 and PVA/ SiO_2 in terms of the physical parameters ΔE, TDM and MESP.

2. Materials and Methods

All calculations were carried out with Gaussian 09 program [26] at Spectroscopy Deparment, National Research Centre. Each structure is optimized with DFT at B3LYP [27-29] together with the basis set LANL2DZ. HOMO-LUMO energy, TDM and MESP were calculated at the same level of theory.

3. Results and Discussion

The reactivity of a given structure was previously reported as a function of some physical parameters such as HOMO-LUMO energy, total dipole moment and the molecular electrostatic potential [30-33]. So, these parameters will be calculated at B3LYP/ LANL2DZ.

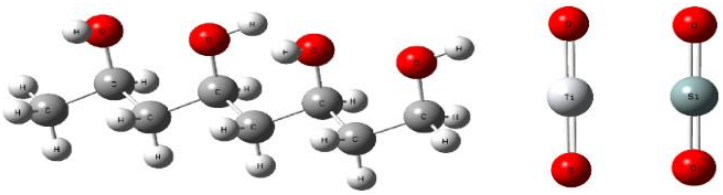

(a) (b) (c)

Figure 1. Optimized structure of a) 4PVA; b) TiO_2 and c) SiO_2.

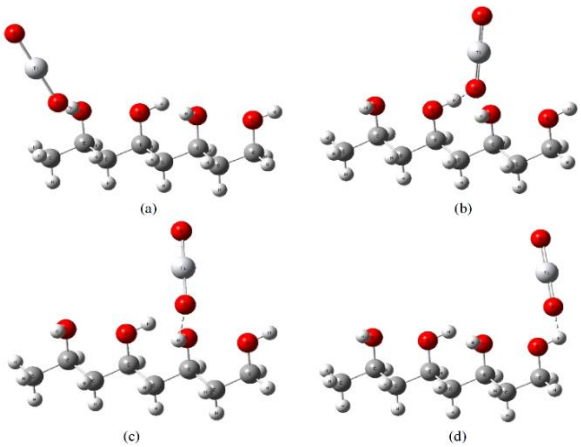

Figure 2. Optimized structure of a) 4PVA-TiO_2 ***P1***; b) 4PVA-TiO_2 ***P2***; c) 4PVA- TiO_2 ***P3*** and d) 4PVA-TiO_2 ***P4***.

It is supposed that the interaction between emeraldine base four units of PVA(4PVA) and 4PVA with TiO_2 and SiO_2 takes place through active sites of 4PVA with different positions. The four different positions are the 4 OH group of 4PVA attached to oxygen atom number: 23; 25; 27 and 29. For each interaction site position, only one probability for the interaction of both TiO_2 and SiO_2 with 4PVA is supposed. Which is, 4PVA-O-X-O where X refers to the titanium and silicon atom. The interaction is supposed to be Van der Waal

interaction. The optimized structures of 4PVA, TiO_2 and SiO_2 are carried out at LANL2DZ level of DFT for more accurate predictions. The optimized structures are shown in figure 1.

However, the supposed structures of 4PVA- O_{23} TiO_2 (4PVA- TiO_2 ***P1***), 4PVA- O_{25} TiO_2 (4PVA- TiO_2 ***P2***), 4PVA- O_{27} TiO_2 (4PVA- TiO_2 ***P3***) and 4PVA- O_{29} TiO_2 (4PVA- TiO_2 ***P4***) are presented in figure 2.

For all structures, the electronic energy gap (HOMO-LUMO), total dipole moment (TDM) and the molecular electrostatic potential are calculated to predict the reactivity of 4PVA as a result of the interaction with TiO_2 and SiO_2 separately.

Table 1. B3LYP/LANL2DZ calculated HOMO-LUMO band gap (ΔE) as eV and TDM as Debye for 4PVA, TiO_2 and 4PVA/TiO_2 nanocomposite at the different interaction sites positions.

Structure	ΔE	TDM
TiO_2	1.9432	0.0000
4PVA	8.1463	3.1058
4PVA-TiO_2 *P1*	1.5508	5.2374
4PVA-TiO_2 *P2*	1.4566	10.6716
4PVA-TiO_2 *P3*	0.7891	5.2085
4PVA-TiO_2 *P4*	0.5685	6.7226

Table 1 presents the changes occurred in the HOMO-LUMO energy (ΔE) and TDM of 4PVA and TiO_2 upon interaction. Where, it is found that 4PVA and TiO_2 possess HOMO-LUMO energy of 8.1463 and 1.9432eV and TDM of 3.1058 and 0.0000 Debye respectively. However, due to the interaction in the four different positions, the values of both physical quantities suffer from a strong change. Where, the HOMO-LUMO energy decreased sharply and becomes 1.5508, 1.4566, 0.7891 and 0.5685 eV for the interaction of TiO_2 with 4PVA throughout the hydrogen atom linked to oxygen atom number 23, 25, 27 and 29 respectively. Such a strong decrease in the HOMO-LUMO energy value of 4PVA refers that it becomes more reactive as a result of interaction with TiO_2. Meanwhile, for the same interaction positions, TDM of PVA increased approximately to twice its value for 4PVA and becomes 5.2374, 10.6716, 5.2085 and 6.7226 Debye instead of 3.1058 Debye. Also, the increase in TDM values of 4PVA upon interaction is considered as a strong indicator for the enhancement of the reactivity of 4PVA.

On the other hand, for the interaction of 4PVA with SiO_2, HOMO-LUMO energy is also calculated and figure 3 presents the optimized structures for 4PVA- O_{23} SiO_2, 4PVA- O_{25} SiO_2, 4PVA- O_{27} SiO_2 and 4PVA- O_{29} SiO_2.

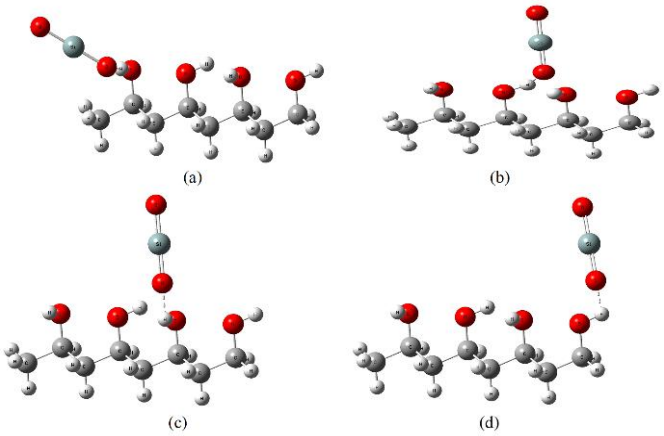

Figure 3. Optimized structure of a) 4PVA- SiO_2 ***P1***; b) 4PVA-SiO_2 ***P2***; c) 4PVA- SiO_2 ***P3*** and d) 4PVA- SiO_2 ***P4***.

Table 2. B3LYP/ LANL2DZ calculated HOMO-LUMO band gap energy (ΔE) as eV and TDM as Debye for SiO_2 and 4PVA/SiO_2 nanocomposite at the different interaction sites positions.

Structure	ΔE	TDM
SiO_2	5.0940	0.0000
4PVA	8.1463	3.1058
4PVA-SiO_2 *P1*	1.7293	5.0978
4PVA-SiO_2 *P2*	3.9941	9.0411
4PVA-SiO_2 *P3*	1.0977	4.4549
4PVA-SiO_2 *P4*	1.0721	6.3546

The calculated values of HOMO-LUMO energy (ΔE) is presented in table 2. Where, the band gap energy of 4PVA decreased to 1.7293, 3.9941, 1.0977 and 1.0721for 4PVA- SiO_2 ***P1***, 4PVA-SiO2 ***P2***, 4PVA-SiO2 ***P3*** and 4PVA-SiO2 ***P4*** respectively instead of 8.1463 and 5.0940eV for 4PVA and SiO_2 respectively.

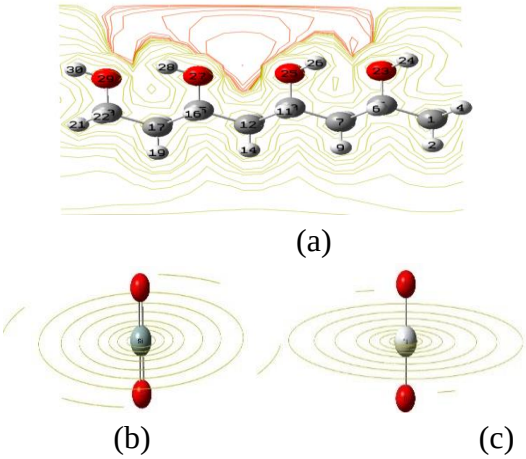

(a) (b) (c)

Figure 4. MESP calculated at B3LYP/LANL2DZ as contour for: a) 4PVA; b) TiO_2 and c) SiO_2.

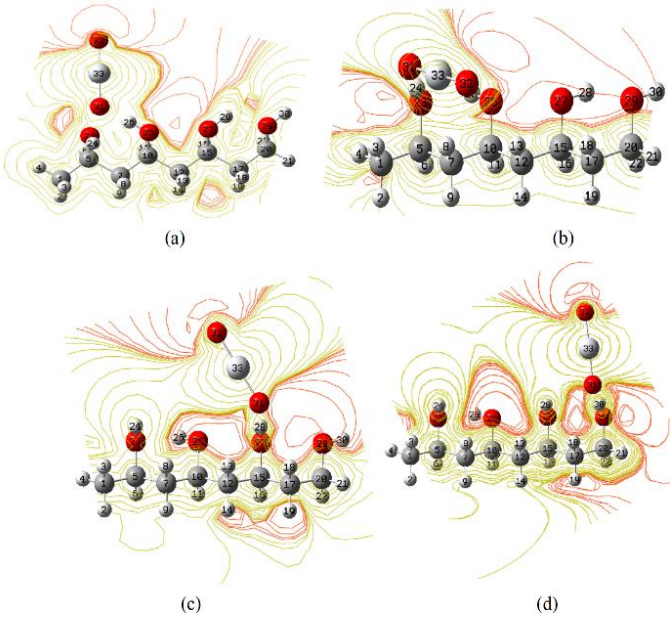

(a) (b) (c) (d)

Figure 5. MESP calculated at B3LYP/LANL2DZ as contour for: a) 4PVA- TiO_2 ***P1***; b) 4PVA-TiO_2 ***P2***; c) 4PVA-TiO_2 ***P3*** and d) 4PVA-TiO_2 ***P4***.

The sharp decrease that occurred in the HOMO-LUMO energy gap of 4PVA and SiO_2 reflects the excellent performance of polymer nanocomposite material in energy storage devices and sensing devices. This behavior of HOMO-LUMO band gap for the nanocomposite material based on 4PVA/ SiO_2 agree very well with the calculated values of TDM. Where, TDM of 4PVA and SiO_2 increased upon interaction from 3.1058 and 0.0000 Debye respectively to 5.0978, 9.0411, 4.4549 and 6.3546 for the interaction of SiO_2 with 4PVA via

the O_{23}, O_{25}, O_{27} and O_{29} of 4PVA. The obtained results of HOMO-LUMO band gap and TDM for the structures representing 4PVA/TiO_2 and 4PVA/SiO_2 reflect the enhancement of the reactivity of 4PVA and hence it's electronic properties.

Furthermore, molecular electrostatic potential (MESP) is also mapped for all structures at B3LYP/LANL2DZ of DFT. The importance of MESP in describing the electronic behavior of polymeric materials comes from the ability of MESP to describe the distribution of electronic charges within the studied molecules. Studying the MESP helps in understanding the electronic configuration and the knowledge of the active sites present within the studied structures. Where MESP can be described by following a color map that started from red color to blue color. The red color refers to the regions very rich with electrons (active sites) while the blue one refers to that who absence of electrons (i.e. inactive sites for interaction). MESP can be mapped as contour, surface and as total density (i.e. 3-dimensional picture).

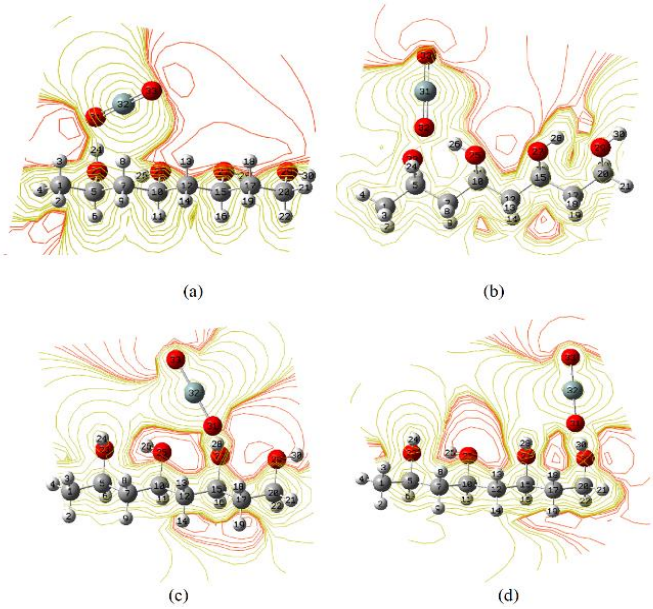

Figure 6. MESP calculated at B3LYP/LANL2DZ as contour for: a) 4PVA-SiO_2 ***P1***; b) 4PVA-SiO_2 ***P2***; c) 4PVA- SiO_2 ***P3*** and d) 4PVA- SiO_2 ***P4***.

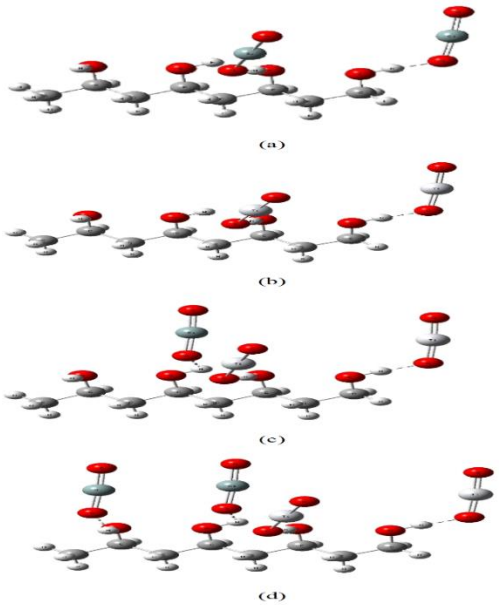

Figure 7. Optimized structure for: a) 4PVA/2TiO_2; b) 4PVA/2SiO_2, c) 4PVA/2TiO_2 /1SiO_2 and d) 4PVA/2TiO_2 /2SiO_2.

Figures 4, 5 and 6 show the calculated MESP as contour for the two nanocomposite systems which are 4PVA/TiO_2 and 4PVA/SiO_2. The figures indicate that the reactivity of 4PVA increased due to the interaction with TiO_2 and SiO_2 as the electro-negativity increased within the structure. Where, as presented in figure 4, that the intensity of the yellow color around the TiO_2 and SiO_2 structures decreased strongly upon interaction with 4PVA. This yellow region refers to the neutral sites within the studied models. This can be understood by looking at the figures, where the red color intensity increased within the 4PVA structure due to the interaction.

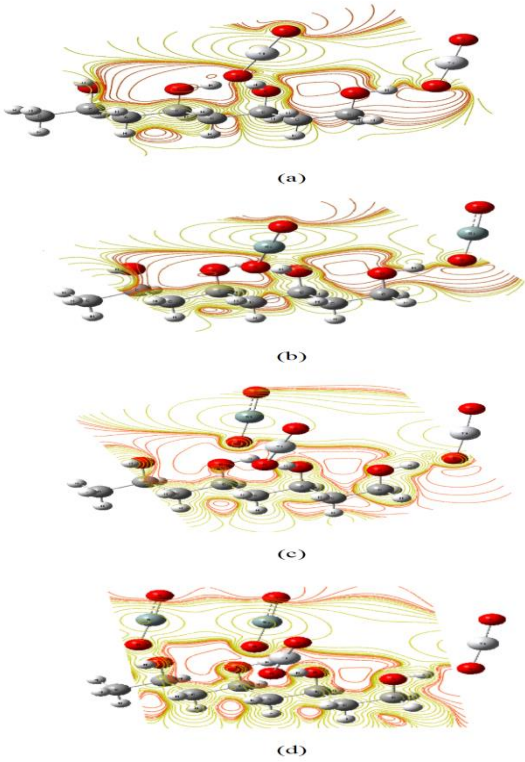

Figure 8. MESP calculated at B3LYP/LANL2DZ as contour for: a) 4PVA/2TiO_2; b) 4PVA/2SiO_2, c) 4PVA/2TiO_2 /1SiO_2 and d) 4PVA/2TiO_2 /2SiO_2.

Table 3. B3LYP/ LANL2DZ calculated HOMO-LUMO band gap as eV and TDM as Debye for 4PVA, with 2TiO_2, 4PVA, with 2SiO_2, 4PVA, with 2TiO_2-1SiO_2 and 4PVA, with 2TiO_2-2SiO_2 nanocomposite at the different interaction sites positions.

Structure	ΔE	TDM
4PVA-2TiO_2	0.5349	5.2086
4PVA-2SiO_2	0.7363	4.9149
4PVA-2TiO_2-1SiO_2	0.5605	7.3735
4PVA-2TiO_2 -2SiO_2	0.6351	12.2711

According to the previous results of HOMO-LUMO energy, TDM and MESP for PVA/ TiO_2 and PVA/SiO_2 structures, the level of calculations can be increased. Where, as the interaction proceeds through position 3 and 4 has the lowest electronic energy gap and they are nearly close, then another class of calculations can be performed by increasing TiO_2 and SiO_2 content to 2 units as presented in figure 7-a and 7-b. Table 3 presents the calculated values of HOMO-LUMO energy and TDM. Where, HOMO-LUMO energy gap decreased to 0.535 and 0.7363 eV for 4PVA/2TiO_2 and 4PVA/2SiO_2 respectively. Meanwhile, TDM does not change significantly where it becomes 5.2086 and 4.9149 Debye for 4PVA/2TiO_2 and 4PVA/2SiO_2 respectively. The decreased values of HOMO-LUMO energy gap confirmed the ability of 4PVA/2TiO_2 and 4PVA/2SiO_2 structures to interact with other nanostructures. Also, it is

noticed from the results that the band gap energy of 4PVA/2TiO_2 is lower than that of 4PVA/2SiO_2. Which confirmed that the surface of 4PVA/TiO_2 is more reactive. So, the addition of other species of nanoparticles is also possible. Where we started another class of model molecule based on 4PVA/2TiO_2/ 1 SiO_2 and 4PVA/2TiO_2/ 2 SiO_2 which are presented in figure 7-c and figure 7-d respectively. Table 3 also presents the effect of adding one and two units of SiO_2 on the properties of 4PVA/2TiO_2. Where the band gap energy and TDM changes to 0.5605 and 0.6351 eV and to 7.3745 and 12.2711 Debye for 4PVA/2TiO_2/1SiO_2 and 4PVA/2TiO_2/2SiO_2 respectively. All these changes in the electronic parameters indicate that there are changes in the distribution of electrons within the studied models. This can be confirmed by the study of MESP for all of them. Figure 8 presents the MESP mapped as contour for 4PVA/2TiO_2, 4PVA/2SiO_2, 4PVA/2TiO_2/1SiO_2 and 4PVA/2TiO_2/2SiO_2. The behavior presents in the figure confirmed that there are fluctuations in the reactivity of the studied structures. Where the intensity of the red color increased for 4PVA/2TiO_2 and 4PVA/2SiO_2. Based on the above results one can conclude that molecular modeling with different levels could be an effective tool for elucidating reactivity and interactions for many systems and molecules in many areas of applications. This is in good agreement with the previous findings [34-40].

4. Conclusions

Molecular modeling at B3LYP/LANL2DZ is performed to study the mechanism of interaction of PVA with TiO_2 and SiO_2. Only one interaction probability is proposed between 4PVA and the nanostructures of TiO_2 and SiO_2 at the different interaction positions. Where the interaction processed through the OH of 4PVA is the most probable to take place. Physical properties such as HOMO-LUMO energy gap, TDM and MESP are calculated at B3LYP/LANL2DZ. Based on the calculated physical parameters, it is concluded that the 4PVA/TiO_2 and 4PVA/SiO_2 and 4PVA-2TiO_2-2SiO_2 polymer nanocomposite materials can be used in developing new materials for sensing devices as the structures seem to be highly reactive. Furthermore, it is concluded that ab-initio methods based on B3LYP/LANL2DZ could be used to follow up the changes occur in the electronic properties, the distribution of charges and the reactivity of polymeric materials.

Funding

This research received no external funding.

Acknowledgments

This research has no acknowledgments.

Conflicts of Interest

The authors declare no conflict of interest.

References

1. Williams, R.J.P.; Fraústo da Silva, J.J.R. *The Chemistry of Evolution*. 2006; pp. 393-414.
2. Saleh, E. *3D and 4D Printing of Polymer Nanocomposite Materials*. 2020; pp. 505-525, https://doi.org/10.1016/C2018-0-01194-9.

3. Hadjab, M.; Ibrir, M.; Berrah, S.; Abid, H.; Saeed, M.A. Structural, electronic and optical properties for chalcopyrite semiconducting materials: ab-initio computational study *Optik* **2018**, *169*, 69-76, https://doi.org/10.1016/j.ijleo.2018.05.044.
4. Kou, J.; Cao, A.; Liu, Z.H.; Gan, L.H. Stability, electronic and mechanical properties of superhard materials formed by 4+6+8 membered rings of carbon. *Journal of Solid State Chemistry* **2019**, *277*, 454-465, https://doi.org/10.1016/j.jssc.2019.06.043.
5. Li, X.H.; Cui, H.L.; Yong, Y.L.; Zhang, R.Z. Elastic, electronic properties and QTAIM of new H-enriched hydrogen storage material Mg(BH4)2·(NH3)2 (NH3BH3). *International Journal of Hydrogen Energy* **2019**, *44*, 7414-7421, https://doi.org/10.1016/j.ijhydene.2018.09.209.
6. Bacha, R.U.S.; Lin, T.T.; Yao, J.; Pan, Q.J. Graphdiyne-actinyl complexes as potential catalytic materials: A DFT perspective from their structural, bonding, electronic and redox properties. *Arabian journal of chemistry* **2020**, *13*, 4564-4576.
7. Badry, R.; El-Khodary, S.; Elhaes, H.; Nada, N.; Ibrahim, M. On the molecular modeling analyses of sodium carboxymethyl cellulose treated with acetic acid. *Letters in Applied NanoBioScience* **2019**, *8*, 553-557, https://doi.org/10.33263/LIANBS 82.553557.
8. El Gabaly, S.G.; Youssif, G.M.; Bayoumy, A.M.; Ezzat, H.; Elhaes, H.; Refaat, A.; Ibrahim, M.A. Modeling The Effect of Functional Groups on The Electronic Properties of Benzene, Pyridine and Pyrimidine, *Egypt. J. Chem. Special issue, the First International Conference on Molecular Modeling and Spectroscopy* **2019**, 1-11, https://doi.org/10.21608/ejchem.2019.12903.1807.
9. Ezzat, H.; Badry, R.; Yahia, I.S.; Zahran, H.Y.; Ibrahim, A.; Elhaes, H.; Ibrahim, M. Mapping the Molecular Electrostatic Potential of Fullerene. *Egyptian Journal of Chemistry* **2019**, *62*, 991-1002, https://dx.doi.org/10.21608/ejchem.2019.5353.1472.
10. Nematov, D.; Burhonzoda, A.; Khusenov, M.; Kholmurodov, K.; Doroshkevych, A.; Doroshkevych, N.; Zelenyak, T.; Majumder, S.; Refaat, A.; Ibrahim, M. Molecular Dynamics Simulations of the DNA Radiation Damage and Conformation Behavior on a Zirconium Dioxide Surface. *Egyptian Journal of Chemistry* **2019**, *62*, 149-161, https://doi.org/10.21608/ejchem.2019.12981.1811.
11. Badry, R.; El-Kohdary, S.; Elhaes, H.; Nada, N.; Ibrahim, M.A. The Influence of Moisture on the Electronic Properties of Monomer, Dimer, Trimer and Emeraldine Base Sodium Carboxymethyl Cellulose, *Egypt. J. Chem. Special issue, the First International Conference on Molecular Modeling and Spectroscopy* **2019**, *62*, 39-56, https://doi.org/10.21608/ejchem.2019.12805.1800.
12. Nematov, D. D.; Burhonzoda, A. S.; Khusenov, M. A.; Kholmurodov, K. T.; Elhaes, H.; Ibrahim, M. A. The Quantum-Chemistry Calculations of Electronic Structure of Boron Nitride Nanocrystals with Density Functional Theory Realization. *Egypt. J. Chem. Special issue, the First International Conference on Molecular Modeling and Spectroscopy* **2019,** *62*, 21-27, https://doi.org/10.21608/EJCHEM.2019.12879.1805.
13. D'Aquino, C.A.; Balmant, W.; Ribeiro, R.L.L.; Munaro, M.; Vargas, J.V.C.; Amico, S.C. A simplified mathematical model to predict PVC photodegradation in photobioreactors. *Polymer Testing* **2012**, *31*, 638-644, https://doi.org/10.1016/j.polymertesting.2012.03.002.
14. Al-Malack, M.H. Migration of lead from unplasticized polyvinyl chloride pipes. *Journal of Hazardous Materials* **2001**, *82*, 263-274, https://doi.org/10.1016/S0304-3894(00)00366-6.
15. Yu, J.; Sun, L.S.; Ma, C.; Qiao, Y.; Yao, H.; Thermal degradation of PVC: a review, *Waste Manag*, **2016**, 48, 300-314. https://doi.org/10.1016/j.wasman.2015.11.041.
16. Huang, J.B.; Li, X.S.; Zeng, G.S.; Cheng, X.C.; Tong, H.; Wang, D.Q.; Thermal decomposition mechanisms of poly(vinyl chloride): a computational study, *Waste Manag*, **2018**, 76, 483-496. https://doi.org/10.1016/j.wasman.2018.03.033.
17. Sun, H.; Cao, B.; Tian, Q.; Liu, S.; Du, D.; Xue, Z.; Fu, H. A DFT study on the absorption mechanism of vinyl chloride by ionic liquids. *Journal of Molecular Liquids* **2016**, *215*, 496-502, https://doi.org/10.1016/j.molliq.2016.01.026.
18. Brydson, J.A. *Plastics Materials.* 6th Edition. Butterworth-Heinemann, USA. 1995.
19. Chopra, S. Electronic properties and optical absorption of graphene-polyvinylidene fluoride nanocomposites:A theoretical study. *Mater Chem Phys* **2017**, *186*, 159-166, https://doi.org/10.1016/j.matchemphys.2016.10.041.
20. Mallakpour, S.; Shafiee, E. The synthesis of poly(vinyl chloride) nanocomposite films containing ZrO2 nanoparticles modified with vitamin B1 with the aim of improving the mechanical, thermal and optical properties. *Des Monomers Polym.* **2017**, *20*, 378-388, https://doi.org/10.1080/15685551.2016.1273436.
21. Kim, S. Pyrolysis kinetics of waste PVC pipe. *Waste Management* **2001**, *21*, 609-616, https://doi.org/10.1016/S0956-053X(00)00127-6.
22. Rajendran, S.; Uma, T. Effect of ZrO2 on conductivity of PVC–LiBF4–DBP polymer electrolytes. *Materials Letters* **2000**, *44*, 208-214, https://doi.org/10.1016/S0167-577X(00)00029-X.
23. Hoherčáková, Z.; Opekar, F. Au/PVC composite—a new material for solid-state gas sensors: Detection of nitrogen dioxide in the air. *Sensors and Actuators B: Chemical* **2004**, *97*, 379-386, https://doi.org/10.1016/j.snb.2003.09.016.

24. Hu, J.; Zhu, Y.; Huang, H.; Lu, J. Recent advances in shape–memory polymers: Structure, mechanism, functionality, modeling and applications. *Progress in Polymer Science* **2012**, *37*, 1720-1763, https://doi.org/10.1016/j.progpolymsci.2012.06.001.
25. Ahmed, R.; Hanan, E.; Nabila, S.A.; Hanan, S.I.; Medhat, I. Green Route for the Removal of Pb from Aquatic Environment. *Combinatorial Chemistry & High Throughput Screening* **2020**, *23*, 1-12, https://doi.org/10.2174/1386207323666200127123349.
26. Frisch, M.J.; Trucks, G.W.; Schlegel, H.B.; Scuseria, G.E.; Robb, M.A.; Cheeseman, J.R.; Scalmani, G.; Barone, V.; Mennucci, B.; Petersson, G.A. Gaussian Inc, Wallingford CT, 2010..
27. Becke, A.D. Density-functional thermochemistry. III. The role of exact exchange. *J. Chem. Phys.* **1993**, *98*, 5648–5652, https://doi.org/10.1063/1.464913.
28. Lee, C.; Yang, W.; Parr, R.G. Development of the Colic-Salvetti correlation-energy formula into a functional of the electron density. *Phys. Rev. B* **1988**, *37*, https://doi.org/10.1103/PhysRevB.37.785.
29. Vosko, S.H.; Wilk, L.; Nusair, M. Accurate spin-dependent electron liquid correlation energies for local spin density calculations: a critical analysis. *J. Phys.* **1980**, *58*, 1200–1211, https://doi.org/10.1139/p80-159.
30. Ibrahim, M.; El-Haes, H. Computational Spectroscopic Study of Copper, Cadmium, Lead and Zinc Interactions in the Environment. *Int. J. Environ. Pollut.* **2005,** *23*, 417-424, http://dx.doi.org/10.1504/IJEP.2005.007604.
31. Ibrahim, M.; Mahmoud, A.A. Computational Notes on the Reactivity of some Functional Groups. *J. Comput. Theor. Nanosci.* **2009**, *6*, 1523-1526, https://doi.org/10.1166/jctn.2009.1205.
32. Politzer, P.; Laurence, P.R.; Jayasuriya, K. Molecular electrostatic potentials: an effective tool for the elucidation of biochemical phenomena. *Environ. Health Persp.* **1985**, *61*, 191-202, https://doi.org/10.1289/ehp.8561191.
33. Şahin, Z.S.; Şenöz, H.I.; Tezcan, H.; Büyükgüngör, O. Synthesis, spectral analysis, structural elucidation and quantum chemical studies of (E)-methyl-4-[(2-phenylhydrazono)methyl]benzoate. *Spectrochim. Acta A* **2015**, *143*, 91-100, https://doi.org/10.1016/j.saa.2015.02.032.
34. Grenni, P.; Caracciolo, A.B.; Mariani, L.; Cardoni, M.; Riccucci, C.; Elhaes, H.; Ibrahim, M.A. Effectiveness of a new green technology for metal removal from contaminated water. *Microchemical Journal* **2019**, *147*, 1010-1020, https://doi.org/10.1016/j.microc.2019.04.026.
35. Afzal, M.A.F.; Hachmann, J. Benchmarking DFT approaches for the calculation of polarizability inputs for refractive index predictions in organic polymers. *Phys. Chem. Chem. Phys.* **2019**, *21*, 4452-4460, https://doi.org/10.1039/C8CP05492D.
36. Ponzoni, I.; Sebastián-Pérez, V.; Martínez, M.J.; Roca, C.; Pérez, C.C.; Cravero, F.; Vazquez, G.E.; Páez, J.A.; Díaz, M.F.; Campillo, N.E. QSAR Classification Models for Predicting the Activity of Inhibitors of Beta-Secretase (BACE1) Associated with Alzheimer's disease. *Sci Rep* **2019**, *9*, 9102, https://doi.org/10.1038/s41598-019-45522-3.
37. Fahim, A.M.; Shalaby M.A.; Ibrahim, M. Microwave-assisted synthesis of novel 5-aminouracil-based compound with DFT calculations. *J. Mol. Struct.* **2019**, *1194*, 211-226, https://doi.org/10.1016/j.molstruc.2019.04.078.
38. Youness, R.A.; Taha, M.A.; Ibrahim, M. In vitro bioactivity, molecular structure and mechanical properties of zirconia-carbonated hydroxyapatite nanobiocomposites sintered at different temperatures. *Materials Chemistry and Physics* **2020,** *239*, https://doi.org/10.1016/j.matchemphys.2019.122011.
39. Badry, R.; Ghanem, A. S.; Ahmed, H.; Fahmy, A.; Elhaes, H.; Refaat, A.; Ibrahim, M. Effect of Li, Na, K, Be, Mg and Ca on the electronic properties, geometrical parameters of carboxylic acids. *Biointerface Research in Applied Chemistry* **2018,** *8*, 3657-3660.
40. Badry, R.; Shaban, H.; Elhaes, H.; Refaat, A.; Ibrahim, M. Molecular modeling analyses of polyaniline substituted with alkali and alkaline earth elements. *Biointerface Research in Applied Chemistry* **2018**, *8*, 3719-3724.